ABCM Symposium Series in Mechatronics - Vol. 1 - pp.635-642
Copyright © 2004 by ABCM

DEVELOPMENT OF A HIGH RESOLUTION UNDERWATER ACOUSTIC POSITIONING SYSTEM

Frederico Vines Faria de Lima
frederico.lima@poli.usp.br

Celso Massatoshi Furukawa
celso.furukawa@poli.usp.br

Escola Politécnica da Universidade de São Paulo – Depto de Engenharia Mecatrônica e de Sistemas Mecânicos
Av. Prof. Mello Moraes, 2231, Cidade Universitária. Cep 05508-900, São Paulo, SP, Brazil

Abstract. *This work presents an ultrashort baseline Acoustic Positioning System for use on underwater vehicles. The position of the vehicle is estimated using time-of-arrival (TOA) estimations of acoustic signals traded between the vehicle and a transponder. Modulated Barker-coded signals are used to achieve low ambiguity. Real-time DSP is implemented in a Programmable Logic Device. The TOA estimator uses a time-domain matched filter with quantized coefficients. The signal design methodology used in this work is described. It is based on the characteristics of the employed acoustic transducers and system requirements. The system was tested using numerical simulation and real acoustic signals obtained in tests performed on a water tank. The results have shown the viability of implementing the proposed APS.*

Keywords. *acoustic positioning system, underwater robotics, offshore equipments.*

1. Introduction

An Acoustic Positioning System (APS) estimates relative positions using acoustic waves (Milne, 1983). For underwater navigation, usually autonomous vehicles carry a two-dimensional array of transducers to receive acoustic signals that are emitted by transponders placed at reference locations. The vehicle sends interrogation pulses to the transponders and measures the time-of-arrival (TOA) of reply signals. The reply is received at the vehicle by the transducer array. The direction-of-arrival (DOA) is estimated computing the relative delays of the TOA measured at the acoustic receivers of the array.

In this case, an Ultrashort Baseline (USBL) APS – where the array baseline usually is shorter than 1 meter, must be used. Since the receiver transducers are placed close to each other, they generate signals with very small phase differences in response to the same arriving signal. In order to obtain TOA estimations of high precision, coded waveforms and signal processing techniques are used.

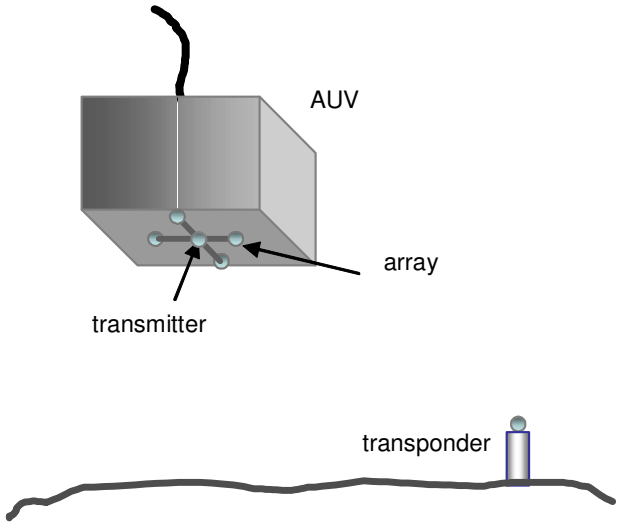

Figure 1. APS for AUV navigation

This work describes an USBL APS that is being developed for guiding an autonomous underwater vehicle (AUV) in missions of retrieval of offshore equipments from the seafloor, as shown in Figure 1. The transponder is placed at the target to be retrieved. The APS is designed for short-range operation (about 100 m), but it must estimate the position with increasing precision as it approaches the target, reaching 50 mm at a distance of 1 m. In this way, the AUV can autonomously connect a rescue tool to the target.

Recently, the development of fast Digital Signal Processors made possible the use of complex waveforms and signal processing for the development of real-time, high accuracy APSs (Austin, 1994; Austin et al, 1997). Further, with the development of commercial high density Field Programmable Gate Arrays (FPGA), fully parallel signal processing is possible. FPGAs have been used for acoustic signal processing and digital communications systems (Ureña et al, 1999; Mukthavaram, 1999), but their use in advanced APS systems has not been reported up to know.

This work describes a configurable APS digital processing unit that performs real-time signal processing using a FPGA. The paper also describes the methodology developed to design the appropriate signal for our specific application. Considerations about the trade-off among criteria like transmitted power, signal length and detection errors are addressed. The signal design methodology employs numerical simulation as a tool in the decision making process.

Finally, main aspects of the system were tested on a water tank. Hemispherical transducers of 114 kHz resonance frequency were constructed and used as transmitter-receiver pair to test the TOA estimation performance and the system.

2. Processing Unit

Figure 2 shows the block diagram of the processing unit. It can sample up to four signals simultaneously and has a high density FPGA to implement digital processing algorithms.

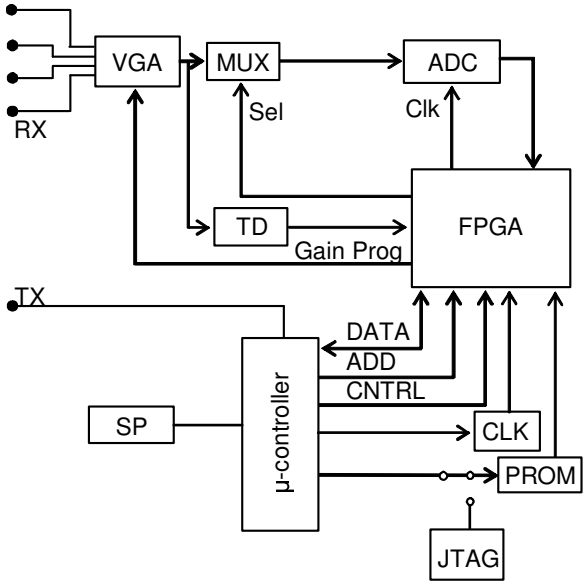

Figure 2. APS processing unit

Input signals (RX) are amplified by a Variable Gain Amplifier (VGA). The FPGA can implement a fixed or a time-variable gain control. In order to sample the four signals with only one A/D converter, a high speed Analog Multiplexer can be used to select the signals cyclically. The 12-bit resolution A/D converter can operate up to 100 MS/s.

Signal processing, storage and other functions are performed by the FPGA. It can operate at high speed, and it has a density of about 600K logic gates. Such characteristics allow the implementation of several signal processing algorithms and logic functions. The FPGA configuration is made with a serial PROM or a JTAG download cable.

A microcontroller controls the whole processing unit. It trades data and instructions with a host computer via a serial port (SP). The microcontroller can also generate digital signals used to drive the acoustic transmitter (TX). The microcontroller uses 3 buses to interface with the FPGA: Data, Address and Control buses. The programmable clock generator (CLK) drives the ADC and the FPGA logic, and is configured by the microcontroller.

The board has also a Threshold Detector (TD) implemented by a voltage comparator. The system can use it to have a coarse TOA estimation. The TD can be connected to one of the VGA outputs, and its output is read by the FPGA.

3. Algorithm implementation

The maximum-likelihood TOA estimator for a known signal with additive white Gaussian noise is the matched filter, which can be defined as a linear system whose impulse response is a replica of the known signal reversed in time (Van Trees, 1968). A matched filter can be approximated by a FIR (Finite-Impulse Response) filter. In order to reduce the computational load necessary to implement this filter, a quantized version of it can be used (Ureña, 1999).

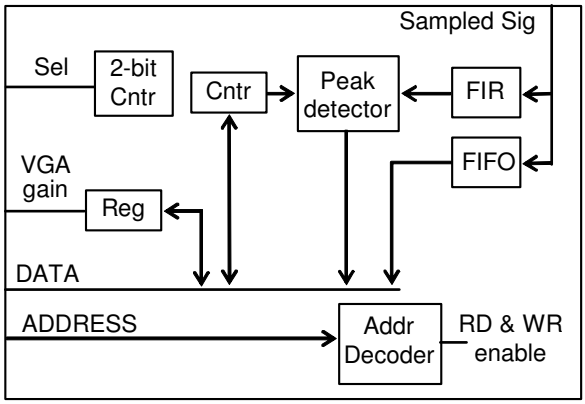

Figure 3. FPGA internal configuration

Figure 3 shows a simplified block diagram of the internal configuration of the FPGA, implementing a matched filter and other logic functions. The sampled signal is filtered by a FIR filter. This filter is generated in the Foundation 4.3 Development System, Xilinx Inc., USA. At the matched filter output, a peak detector searches the signal peak within a predefined time window. A counter (Cntr) is used to count the number of sampling cycles and control the peak detector. The FPGA contains a register (Reg) that supplies the VGA gain, and a 2-bit counter that controls the input multiplexer.

In this configuration, the FPGA also implements a fast FIFO memory that stores the raw sampled signal, in order to allow the off-line processing of the signal for comparison.

4. Piezoelectric transducers

Some hemispheric transducers were assembled for the APS. Figure 4 shows a schematic representation of one transducer.

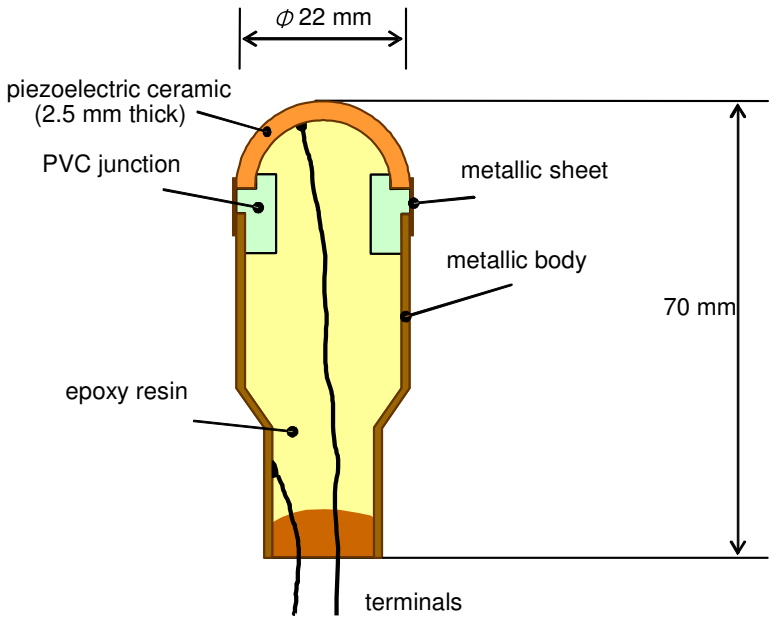

Figure 4. Hemispheric piezoelectric transducer

The piezoelectric component is a PZT-5A hemispheric ceramic with diameter of 22 mm and 2.5 mm thick, Morgan Matrox Inc., UK. The hemispheric shape provides a very low directivity. This is required for underwater navigation. One electric terminal is soldered directly to the internal metallized surface of the ceramic, while the other terminal is soldered to the metallic body of the transducer, which is in electrical contact with the external metallized surface of the ceramic. The transducer body is filled with epoxy resin, which constitutes the backing. The resin also binds the pieces together, provides insulation to the electric contacts and allows the transducer to operate at high pressure.

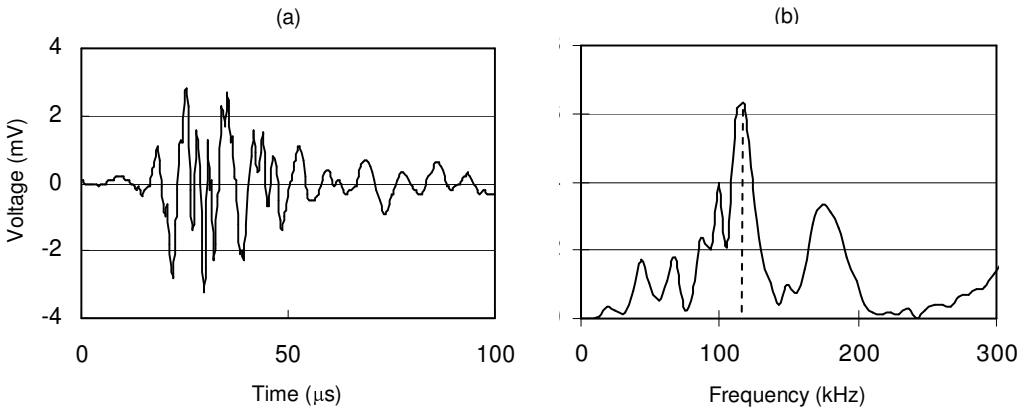

Figure 5. (a) Impulse response of a transmitter-receiver pair; (b) FFT of the impulse response

The impulse response of a transmitter-receiver pair of transducers was obtained experimentally (Fig. 5.a). Two transducers were placed front-to-front about 0.15 m apart in a small water tank. A short pulse, amplified by a wideband power amplifier, was applied to one transducer. The signal received by the other transducer corresponds approximately to the impulse response of the transducer pair. The signal was adjusted in order to correspond to a transmitter-receiver pair separated by 1 m. This impulse response was used to synthesize signals for use in numerical simulations. Figure 5.b shows the FFT of the impulse response shown in Fig. 5.a. The dashed line indicates the frequency that yields the highest power transmission (approximately 114 kHz). This frequency was chosen as the carrier frequency of the transmitted signals.

5. Signal design and simulations

To achieve low uncertainty levels of the TOA estimation, acoustic signals with BPSK modulation using Barker codes are employed (Van Trees, 1971). Table 1 shows the known Barker codes.

The longer known Barker code has 13 bits and one can expect that it will provide the lowest uncertainty. Also, signals with long duration result in more transmitted acoustic power, raising the intensity of the signal that reaches the APS transducers. However, long signals must be avoided in the present application for three reasons. First, the FIR filter would have too much coefficients and could not fit the FPGA. Second, the reply signal must be as brief as possible to save battery power of the transponder. And third, when the vehicle is close to the transponder, the APS array can receive multipath signals.

Table 1: Known Barker Codes (N: number of bits)

N	Code
2	-1 1
3	1 1 -1
4	1 1 -1 1
5	1 1 1 -1 1
7	1 1 1 -1 -1 1 -1
11	1 1 1 -1 -1 -1 1 -1 -1 1 -1
13	1 1 1 1 1 -1 -1 1 1 -1 1 -1 1

Keeping the modulating frequency constant, which is imposed by the resonance frequency of the ultrasonic transducers, shorter signals can be achieved choosing a Barker code with few bits, or raising the baud rate of the transmission. In the case of BPSK modulation, the baud rate can be increased transmitting less cycles of the carrier signal per coded bit.

Therefore, there is a trade-off between choosing a long signal – with many bits and many carrier cycles per bit, or a brief one. The criterion adopted in this work is to select a signal that:

1. Provides a low uncertainty level
2. As short as possible to save battery power and FPGA space
3. Provides a good energy transfer

As for the energy of the signal, many cycles yield a better choice. This aspect was investigated simulating the relative energy transmission with a transducer pair, for different types of signals. The signal energy can be defined as:

$$E = \sum_{n=1}^{N} s^2[n], \tag{1}$$

where s[.] are the signal samples and N is the number of samples.

To simulate the transmission and the reception of the acoustic signals, it was used the impulse response of the transmitter-receiver pair of transducers (measured experimentally, as explained before). Each signal was synthesized applying to this impulse response a 114 kHz binary signal modulated with one Barker code. This procedure was repeated for each of the seven known Barker codes.

The energy transmission was calculated as the ratio between the energy of the received signal and the energy of the excitation signal. Figure 6 shows a graph comparing this measure for different signals. For a better comparison, the values were calculated in dB relatively to the maximum obtained value using the following expression:

$$TdB_i = 10 \cdot \log_{10} \frac{T_i}{T_{\max}}, \tag{2}$$

where T_i is the transmitted energy of the i-th signal, T_{max} is the maximum transmitted energy obtained among all tested signals, and TdB_i is the relative energy transfer in dB. It was observed that above five cycles per coded bit, the relative energy transmission increases only slightly.

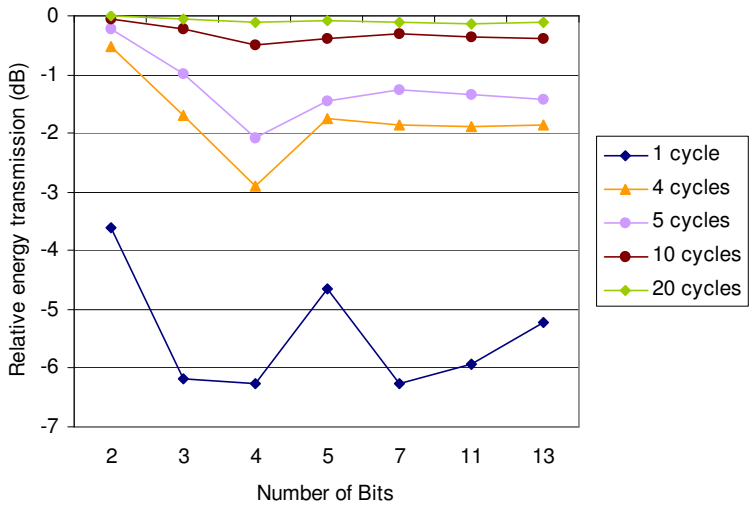

Figure 6: Relative energy transmission evaluation for signal design

To investigate the deviation achieved with different signals, the TOA estimator was simulated using synthesized signals corrupted with Gaussian noise for SNR = 2. Figure 7 illustrates the process of generation of synthesized signals. For each signal type, it was generated a set of 1,000 signal samples. For each set, it was determined the standard deviation of TOA estimations.

The SNR was defined according to Eq. (3).

$$SNR = \frac{\frac{1}{N}\sum_{n=0}^{N-1} s^2[n]}{\sigma_N^2}, \tag{3}$$

where s[.] are the signal samples, N is the number of samples, and s^2_N is the adopted level of noise power.

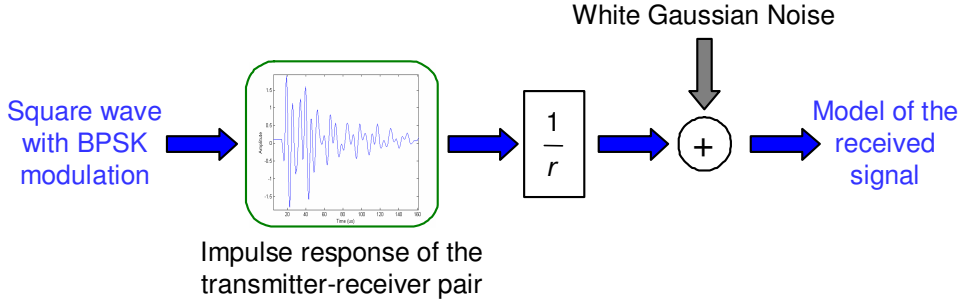

Figure 7. Generation of synthesized signals

Figure 8 shows the obtained deviation for some signal types. As expected, a signal with high baud rate (i.e. few cycles per bit) provides low uncertainty, since the bandwidth of the signal increases. However, such a signal yields a low energy

transmission level. Accepting a deviation of about 0.5 µs, one can select the signal with 5 bits and 5 cycles per bit. Since the ADC samples the signal at 2 MS/s per channel, the resolution of the TOA estimator is 0.5 µs. Therefore, a deviation below 0.5 µs is not necessary. Further, such TOA error corresponds to a direction error of less than 0.05 degrees (considering two transducers separated by 1 m, 100 m away from the transponder).

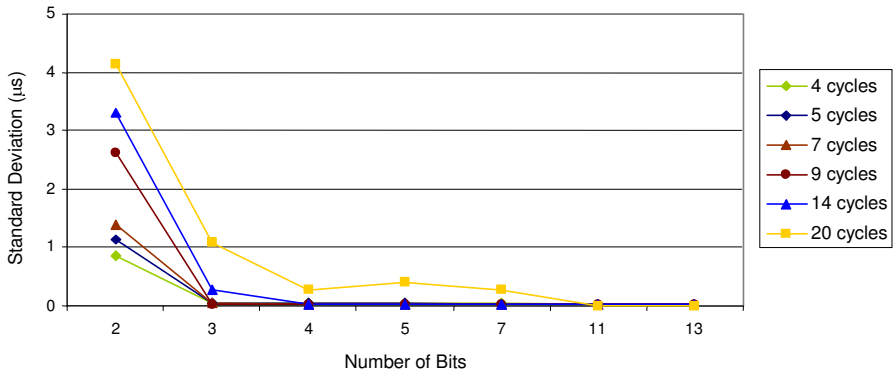

Figure 8: Standard deviations of TOA estimations

6. Experimental tests

In order to verify the transducers response and the performance of the algorithms for real signals, experimental tests were conducted in a water tank, with 25 m of length, 1 m wide and 1 m deep.

Figure 9 shows the experimental setup of the experiment. The transducers were mounted on holding structures. A personal computer (PC) with an ADC and a DAC boards controlled the whole experiment. A square BPSK modulated signal generated by the DAC board was amplified by a linear power amplifier and applied to one transducer. The output of the DAC also was used to trigger the acquisition board. The ADC board acquired the signals received by the other transducer. The received signals were observed with an oscilloscope for verification.

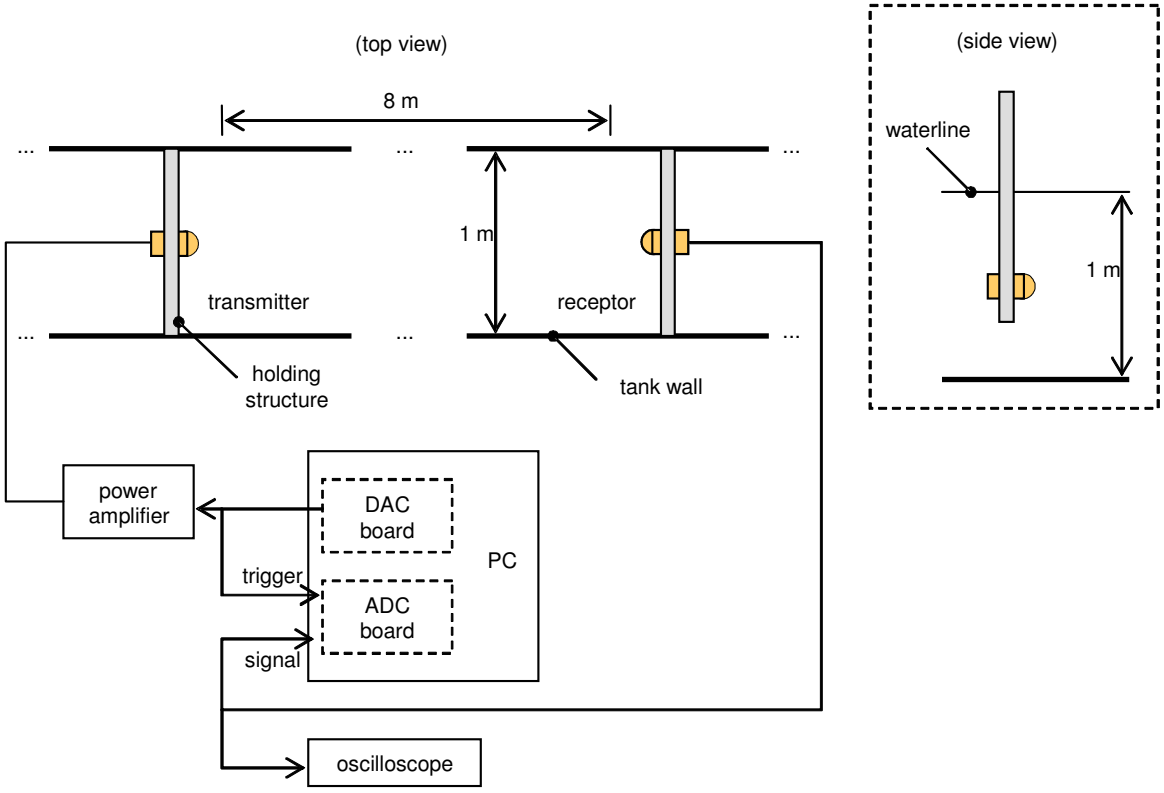

Figure 9. Experimental setup for signal generation and acquisition

The used signals have a 114 kHz carrier frequency with BPSK modulation using the 5-bit Barker code and 5 cycles per bit. Figure 10.a shows the mean of 100 received signals sampled with the transducers separated by 0.2 m. This signal

was used as the reference signal in TOA estimations.

The transducers were placed 8 m apart, and received signals were sampled and stored at the PC's memory. Figure 10.b shows one example of a received signal. We can observe a strong multipath effect due the relatively small tank width and deepness. Two sets of 100 signals were stored, using two different noise levels. The noise power levels were 10 % and 40 % of the received signal power level. The amplification of the DAC output was adjusted in order to produce these two different signal-to-noise ratios.

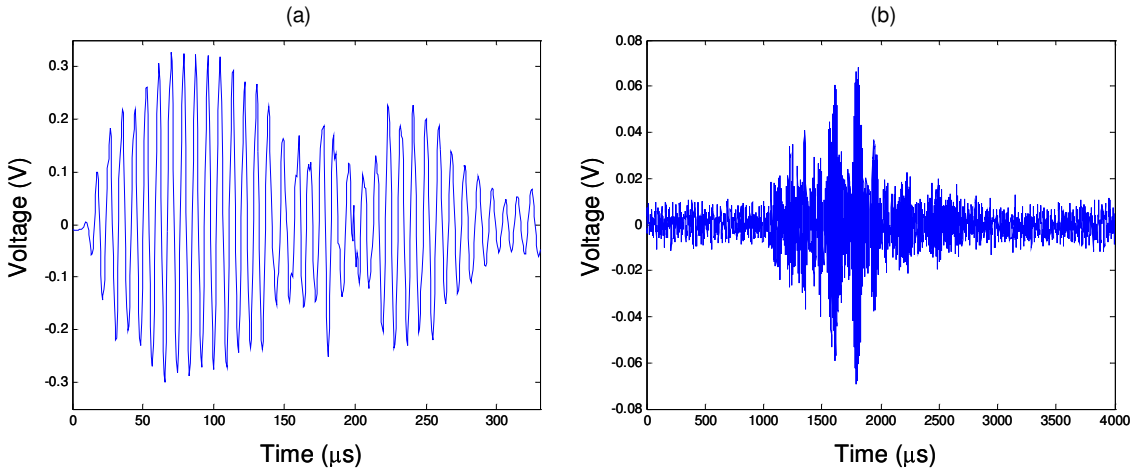

Figure 10-. Experimental signals: (a) reference signal, obtained in very short distance; (b) signal + noise (10 %), and with transducers separated by 8 meters

The signals were processed with a matched filter using as reference the signal obtained at a short distance, as explained before. The standard deviations of the TOAs were 1 μs at 10 % of noise and 6 μs at 40 % of noise. Figure 11 shows the TOA of 34 signals at 40 % of noise. In this case, the major variations around the media of 6465 μs were of about 9 μs, which is close to the carrier period, and suggests that the matched filter found the output maxima in adjacent peaks.

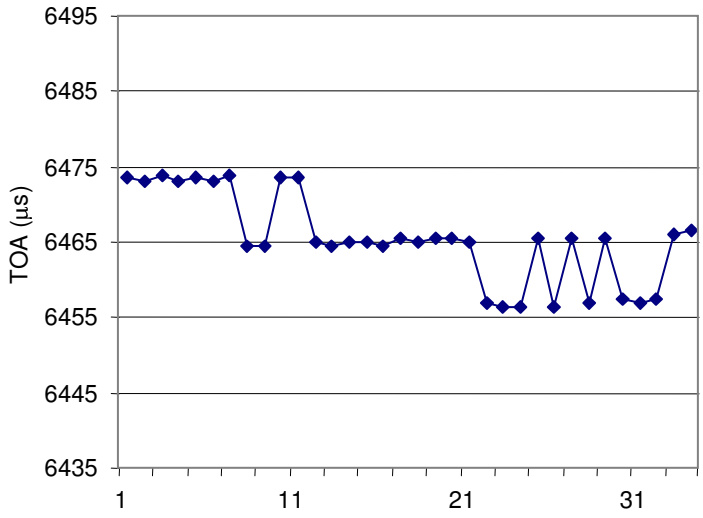

Figure 11. Time-Of-Arrival of 34 acquired signals with noise level of 40 %

Measured deviations are higher than the level that was predicted by the simulations. It must be observed that simulated model does not include multipath effects, that was significative in our experiments, due to the small dimensions of the available water tank. As one can see from Fig. 10.b, multipath signals result on noise levels much larger than background noise level observed in the experiments. The multipath noise has power level with the same order of the signal power. Under such high noise condition, the deviation of TOA estimations using matched filter is no longer linear (Van Trees, 1968). The error corresponds to the false detection of lateral peaks of the filter output. The cross-correlation of modulated signals produces peaks separated by the carrier period. This is the result observed in the Fig. 11. Sources of multipath signals must be investigated and tests on a larger tank are going to be performed to avoid this problem.

However, the matched filter was able to estimate TOAs with a deviation of only 1 μs, even under severe noise condition. New experiments must be conducted under better conditions of tank dimensions and electronic noise rejection.

7. Conclusions

The proposed APS processing unit provides high programmability, flexibility and can be used in many other applications, like non-destructive testing and acoustic communications. The use of high density FPGA allows the implementation of real-time DSP algorithms.

The design of the signal used by the APS considered the trade-off between short and long signals. Short signals provide better TOA estimation, but produce lower transmitted power. On the other hand, long signals must be avoided to save battery power and FPGA space.

Experimental results have shown the good algorithm performance with transducers separated by 8 m in a multipath environment. Transducers tests have verified its suitability to the application.

8. Acknowledgements

The authors acknowledge the Brazilian agencies CNPq and FINEP for financial support, and Xilinx, Inc., USA, for software donation.

9. References

Austin, T.C., 1994, “The application of spread spectrum signaling techniques to underwater acoustic navigation”, Proceedings of AUV’94 Conference, Cambridge, USA, p.443-449.

Austin, T.C. et al, 1997, “RATS - a relative acoustic tracking system developed for deep ocean navigation”, Proceedings of MTS/IEEE Oceans’97, New York, USA, vol. 1, p. 535-540.

Milne, P.H., 1983, "Underwater Acoustic Positioning Systems", Gulf Pub. Co., Houston, USA, 284 p.

Mukthavaram, S., 1999, "Design and Implementation of an Adaptive Demodulator", Master Thesis, University of Kansas, USA. Available online at <www.ittc.ukans.edu/projects/ACS/documents>

Ureña, J. et al., 1999, “Correlation detector based on a FPGA for ultrasonic sensors”, Microprocessors and Microsystems, vol. 23, pp. 25-33.

Van Trees, H.L., 1968, "Detection, Estimation, and Modulation Theory - Part I", John Wiley, New York, USA, 697 p.

Van Trees, H.L., 1971, "Detection, Estimation, and Modulation Theory - Part III", John Wiley, New York, USA, 627 p.